Surface Characterization of Cu−M (M = Ti, Zr, or Hf) Alloy Powder Catalysts

Árpád Molnár*

Department of Organic Chemistry, József Attila University, Dóm tér 8, H-6720, Szeged, Hungary

Imre Bertóti and János Szépvölgyi

Research Laboratory of Materials and Environmental Chemistry, Chemical Research Center, Hungarian Academy of Sciences, P.O. Box 17, H-1525, Budapest, Hungary

Gabriele Mulas and Giorgio Cocco

Dipartimento di Chimica, Universitá di Sassari, Via Vienna 2, I-07100 Sassari, Italy

Received: May 12, 1998

X-ray photoelectron spectroscopy was used for surface characterization of amorphous Cu−M alloy powders ($Cu_{40}Ti_{60}$, $Cu_{50}Zr_{50}$, and $Cu_{65}Hf_{35}$) produced by mechanical alloying of the constituents. When used as catalyst in the dehydrogenation of alcohols Cu−Zr and Cu−Hf were found to undergo structural changes resulting in surface copper enrichment with a substantial fraction of copper being in fully reduced, metallic (Cu^0) state. This result accounts for the high and stable catalytic activity of Cu−Zr and Cu−Hf in the transformations of alcohols. In contrast, when Cu−Ti is used in inert atmosphere, surface enrichment of titanium is observed. Although segregation of copper occurs in the presence of hydrogen, only oxidized copper species are detected on the surface. In either case, the catalytic activity of Cu−Ti is inferior to the other two alloy samples. TiH_2 is shown by XRD to be the characteristic species formed under hydrogen. This is stable in the presence of hydrogen and, therefore, Cu acts as an oxygen scavenger and forms oxidized surface species that do not show catalytic activity.

Introduction

It has been found in a recent study[1] that copper-containing bicomponent amorphous alloy powders produced by mechanical alloying undergo in situ activation when applied as catalyst in the transformation of various alcohols at elevated temperature (523−573 K). In the dehydrogenation of 2-propanol to acetone and in the transformation of allyl alcohol to form propanal and 1-propanol, active, stable, and selective catalysts are generated from Cu−Zr and Cu−Hf. DSC and XRD data indicated bulk crystallization. Measurement of Cu^0 surface area and preliminary XPS studies showed copper segregation to the surface. Cu−Ti, in contrast, exhibited negligible activity, and its surface features were different from those of the other two alloys. Here the results of a detailed study with respect to the surface characteristics of all three copper alloy catalysts are reported. An attempt is also made to rationalize their catalytic behavior on the basis of surface features.

Experimental Section

Materials. Copper (−150 mesh, 99.5%, impurities in ppm: Sn 130, Fe 100, Ca 40, Si 25, Ag 15, Mg 15, Ni 15, Zn 10, Co 4, Zr 3), titanium (−100 mesh, 99.9%, impurities in ppm: Zr 130, Cr 120, Al 55, Ni 40, Ca 15, Mn 12), and hafnium (−325 mesh, 99.5%, contains 3.5% zirconium, impurities in ppm: O 620, N 120, C <30, Nb <50, Ta <100, Fe <200) powders were purchased from Aldrich, whereas zirconium powder (−20 + 60 mesh, 99.9%, impurities in ppm: Al 50, Fe 750) was an Alfa product.

Methods. The amorphous alloy powders were obtained by mechanical alloying of the elemental powders in argon atmosphere by using a Spex-Mixer Mill (model 8000). The nominal composition in atomic percent of the alloy samples prepared by mechanical alloying is $Cu_{40}Ti_{60}$, $Cu_{50}Zr_{50}$, and $Cu_{65}Hf_{35}$. The resulting materials were characterized by X-ray diffraction (XRD; Siemens D500 and Rigaku D/Max equipments) and differential scanning calorimetry (DSC; Perkin-Elmer DSC 2 equipment). Results of these measurements can be found in a recent publication.[1]

XP spectra were recorded by a Kratos XSAM 800 spectrometer using either Mg $K\alpha_{1,2}$ radiation or Al $K\alpha_{1,2}$ (for Zr-containing samples) with fixed analyzer transmission mode. Wide-scan spectra recorded for identification of the constituents and impurities were acquired with 0.5-eV steps while region spectra with 0.1-eV steps applying 80 and 40 eV pass energy, respectively. The most intense characteristic lines of the constituents, namely, Cu2p, Cu(LMM), Ti2p, Zr3d, and Hf4d regions were taken for the respective samples; O1s and C1s lines for impurities were recorded for each sample.

The pressure in the sample analysis chamber was lower than 10^{-7} Pa. The spectra were referenced to the C1s line (284.8 eV BE) of the CH_x type surface impurity. Data acquisition and processing, including quantification, were performed with the Kratos Vision 2000 data system.

The relative amount of different oxidation states of Ti, Zr, and Hf was determined by fitting the recorded line shape of Ti2p, Zr3d, and Hf4d doublets by mixed Gaussian with 20%

* To whom correspondence should be addressed. Tel: (36) 62-454-277. Fax: (36) 62-322-668. E-mail: amolnar@chem.u-szeged.hu.

10.1021/jp982209t CCC: $15.00
Published on Web 10/21/1998

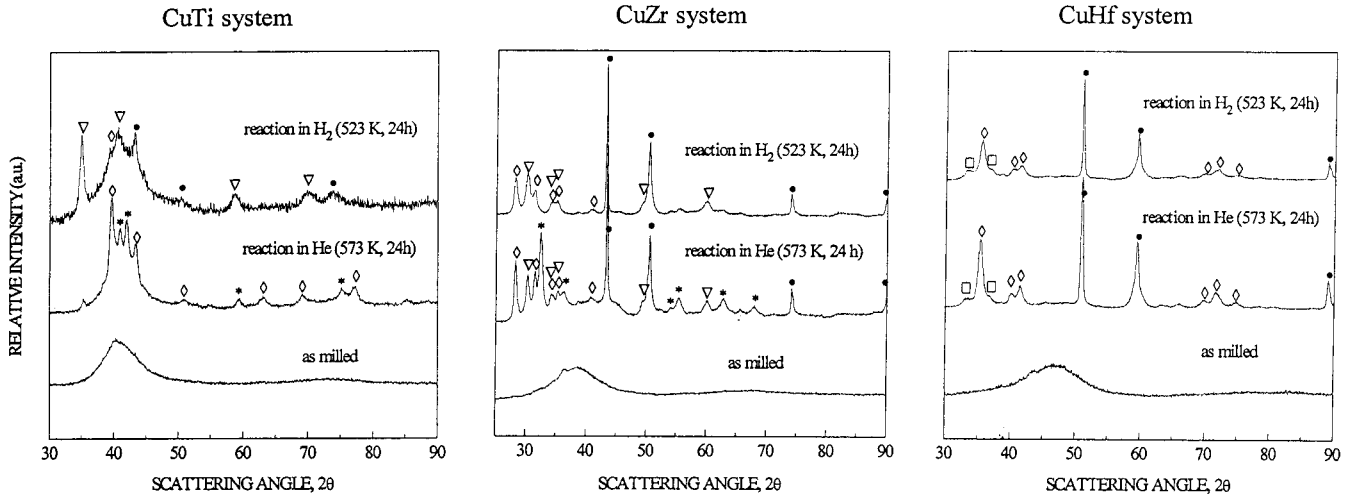

Figure 1. XRD patterns of the Cu−M samples as prepared by mechanical alloying and after catalytic runs performed in helium or hydrogen. Symbols refer to the crystalline phases observed after the catalytic tests and corresponds to the JCPDS quoted files. Cu−Ti (λ = Cu Kα): ●, Cu (4−836) ▽, TiH_2 (9−371) ◇, $CuTi_2$ (15−717) *, γ-CuTi (7−114); Cu−Zr (λ = Cu Kα): ●, Cu (4−836) ◇, m-ZrO_2 (36−420) ▽, tetra-ZrO_2 (17−923) *, ZrH_2 (17−314); Cu−Hf (λ = Co Kα): ●, Cu (4−836) ◇, HfO_2 (8−342) □, HfO_2 (6−318).

Lorentian synthetic components fixing the theoretical intensity ratios at 2:1 and 3:2 for the p and d lines, respectively. Energy separation of the component lines was taken from the literature.[2,3] The line widths at half-maximum of the peak intensity at the applied resolution were in the range of 1.7−1.9 eV, and about 10−20% of lifetime broadening was allowed for the lower quantum state components ($2p_{1/2}$, $3d_{3/2}$, and $4d_{3/2}$).

A different approach was applied for fitting the inherently complex line shapes of the Cu2p and Cu(LMM) spectra of the catalysts where the presence of all three oxidation states of copper could be anticipated. Spectra of both lines were recorded previously on well-defined samples of metallic Cu, Cu_2O, and CuO and were stored as representative "model" spectra. These spectra contain the entire features characteristic of the three chemical states, i.e., the width and asymmetry of the lines, the shake-up satellites, etc., representative also for the applied experimental conditions. These model spectra were used as components for the synthesis of the Cu2p and Cu(LMM) spectra recorded for the catalysts.

The Cu^0 surface area of the catalysts was measured by N_2O titration based on the reaction of nitrous oxide with Cu^0 species using the GC pulse method.[4,5]

Results

Crystallinity. As it has been shown in our previous study, all three alloy samples were amorphous by XRD in their initial, as-received state and underwent crystallization during catalytic reactions in helium.[1] Representative XRD patterns are now reported in Figure 1 where traces of the as-prepared powders as well as those recorded after reactions in the presence of helium or hydrogen are shown.

After using the amorphous Cu−Zr and Cu−Hf powders in the dehydrogenation reaction of 2-propanol in helium (573 K, 24 h), the most significant change is the appearance of elemental copper. In addition, the XRD spectra showed the presence of zirconium hydride, zirconium oxides, and hafnium oxides in the respective samples. In a sharp contrast, when Cu−Ti was subjected to identical conditions, no segregation of the metallic Cu occurred. Instead, $CuTi_2$ and γ-CuTi intermetallic phases were formed.

The uppermost patterns in Figure 1 show the structural reconstructions occurring when the reactions were carried out in hydrogen carrier gas (523 K, 24 h). In the case of Cu−Zr and Cu−Hf powders, demixing of Cu from the amorphous matrix was the predominant process together with the formation of the zirconium and hafnium oxides. It is of interest to note that the formation of the ZrH_2 phase, which was observed in helium, appeared now to be of minor significance. In contrast, in the case of Cu−Ti, an important contribution of the scattering intensity comes from a residual amorphous fraction. Even though signals pertaining to elemental Cu are discernible, the main crystalline peaks in the pattern are due to TiH_2.

TABLE 1: Changes in Cu^0 Surface Area ($m^2\ g^{-1}$) of Cu−M Amorphous Powders (As Measured by N_2O Titration) Induced by Hydrogen Treatment and Reaction[a]

alloy sample	after hydrogen treatment (563 K, 24 h)	after reaction (523 K, 24 h)		
		allyl alcohol in H_2	2-propanol in He	2-propanol in H_2
$Cu_{40}Ti_{60}$	—[b]	—[b]	—[b]	—[b]
$Cu_{50}Zr_{50}$	0.18	0.84	0.45	4.60
$Cu_{65}Hf_{35}$	0.22	0.30	0.20	1.88

[a] Sample size, 100 mg; flow rate of helium, 8 mL min^{-1}; flow rate of hydrogen, 20 mL min^{-1}. [b] Unmeasurably low.

Cu^0 Surface Area and Catalytic Activity. The amount of Cu^0, measured by N_2O titration and represented as Cu^0 surface area in Table 1, was very low not only for the as-received state of Cu−Zr and Cu−Hf alloy powders but also after their treatment in hydrogen. When these alloys were used in the presence of hydrogen for the transformations of allyl alcohol (to form propanal and 1-propanol) and of 2-propanol (to form acetone through dehydrogenation), a significant increase in the Cu^0 surface area occurred. The increase was much more pronounced in the transformation of 2-propanol, indicating that not only the hydrogen in the reaction mixture but the reaction itself also affects the structural and chemical changes taking place on the surface of Cu−Zr and Cu−Hf samples. In contrast, the quantity of Cu^0 was always unmeasurably low for Cu−Ti regardless of pretreatment and reactions applied (Table 1).

In harmony with these observations, substantial changes in the catalytic activity of the alloy powders were observed. In helium, the activity of all three alloys was rather low and even diminishing during the reaction (Table 2). In hydrogen, in contrast, Cu−Zr and Cu−Hf either exhibited a marked increase in activity (Table 2, the transformation of 2-propanol) or

TABLE 2: Rate Data (mol g_{cat}^{-1} s^{-1} 10^{-6}) of Transformation of 2-Propanol and Allyl Alcohol over Cu−M Powders

	2-propanol in He[a]		2-propanol in H_2[b]		allyl alcohol in H_2[c]	
	I	F	I	F	I	F
$Cu_{40}Ti_{60}$	0.2	0.4	1.6	1.3	10.0	0.2
$Cu_{50}Zr_{50}$	3.6	3.0	1.4	14.3	13.1	15.6
$Cu_{65}Hf_{35}$	2.6	0.8	3.0	10.2	15.4	14.9

[a] 30 mg of catalyst, 523 K, 8 mL min^{-1} helium. [b] 30 mg of catalyst, 523 K, 20 mL min^{-1} hydrogen. [c] 30 mg of catalyst, 573 K, 20 mL min^{-1} hydrogen. I, initial rate calculated at 0.5 h time on stream. F, final rate calculated at 10 h time on stream.

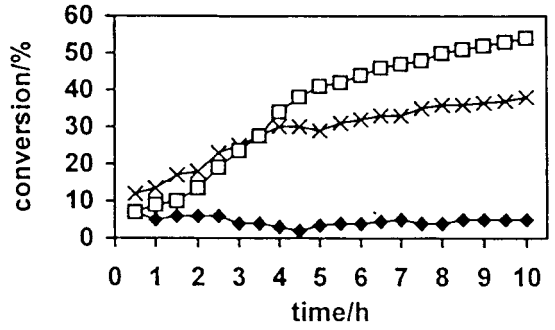

Figure 2. Changes in the catalytic activity of the Cu−M alloy powders in the dehydrogenation of 2-propanol as a function of time on stream (523 K, 20 mL min^{-1} hydrogen) (◆, Cu−Ti; □, Cu−Zr; ×, Cu−Hf).

TABLE 3: Cu to M Atomic Ratios of Cu−M Alloy Powders and Hf to Zr Ratios of the Cu−Hf Alloy

			on surface		
		in bulk (nominal)	as received	after reaction in helium[a]	after reaction in hydrogen[b]
$Cu_{40}Ti_{60}$	Cu/Ti	0.67	1.4	0.2	2.2
$Cu_{50}Zr_{50}$	Cu/Zr	1.0	0.7	1.1	2.2
$Cu_{65}Hf_{35}$	Cu/(Hf + Zr)[c]	1.86	0.6	0.7	5.1
	Hf/Zr	14	0.5	0.2	3.4

[a] 100 mg of sample, 2-propanol, 573 K, 8 mL min^{-1} helium, 24 h. [b] 100 mg of sample, 2-propanol, 523 K, 20 mL min^{-1} hydrogen, 24 h. [c] Due to the segregation of zirconium impurity to the surface, values were calculated by using the sum of Hf and Zr.

displayed high and stable activity throughout the catalytic process (Table 2, the transformation of allyl alcohol). The activity of Cu−Ti, however, was always very low, and also in the transformation of allyl alcohol the originally high activity rapidly diminished (Table 2). Characteristic changes in the catalytic activity of the alloy powders in the dehydrogenation of 2-propanol are given in Figure 2.

Evaluation of the Surface Composition. The results of the quantitative evaluation of the surface composition were obtained on the basis of area intensities of O1s, C1s, Cu2p, Ti2p, Zr3d, and Hf4d lines using the kinetic energy-corrected relative photoionization cross section data (i.e., sensitivity factors) for F.A.T. mode provided within the KRATOS Vision 2000 software package: 0.660 for O1s, 0.250 for C1s, 6.300 for Cu2p, 1.800 for Ti2p, 2.100 for Zr3d, and 2.120 for Hfd4. Since no reliable information on the layered nature of the surface of the particles exists, the simplest, bulklike approach was applied.

Surface Composition Changes. Data on the surface composition of the alloys induced by the catalytic reaction in helium or hydrogen are presented in Table 3 as copper-to-metal ratios. The expected nominal bulk values of the as-prepared alloys are also indicated. The latter were calculated assuming homogeneous distribution of the constituents. The actual concentrations of the alloying elements and that of oxygen and carbon impurities are given in Table 4.

It was observed that in all cases the concentration of copper on the surface is rather low due to oxygen and carbon impurities (Table 4). In addition, the ratio of the concentration of copper to the alloying components on the surface in the as-received state differs substantially from the nominal bulk composition (Table 3). The amorphization process results in a copper-rich surface in the case of Cu−Ti, whereas copper depletion on the surface is characteristic of Cu−Zr and Cu−Hf.

The behavior of Cu−Ti, again, is different when used as a catalyst in the presence of helium in the dehydrogenation of 2-propanol. A marked drop in surface copper concentration is observed, in contrast with Cu−Zr and Cu−Hf, which display copper enrichment. Finally, all three alloys exhibit a marked increase in surface copper concentration when the transformation of 2-propanol is carried out in the presence of hydrogen. This change is especially pronounced for Cu−Hf. XPS revealed an additional interesting feature. Hafnium powder used in mechanical alloying contained a few percent of zirconium that segregated to the surface during ball milling. Further zirconium enrichment occurred during the reaction in helium. After catalytic reaction in hydrogen environment, segregation of zirconium became less pronounced.

On the Effect of Surface Contaminations. It is known that the results of XPS analysis are significantly affected by surface contaminations due to exponential attenuation of the signals by the outermost contaminant layers. In the case of well-defined surface morphology (plain surface, spherical particles, etc.), this effect can be estimated to a certain accuracy. This accuracy, however, is not very high because of the usually unknown composition density and packing of the contaminant layer.

In our case, the preparation of the samples and also their structural and surface chemical transformations in association with the change in atomistic morphology and the possibly graded nature of the alloying components and the covering oxide layers brought about so many uncertainties that no treatments involving layered surface models were attempted. Table 4 gives a guide of the carbon and oxygen contamination of the samples. The dominant chemical state of the carbon is hydrocarbon type with a few percent of C−O, carboxylic, and carbonate type carbon. It is not known whether this contaminant layer is of equal thickness on various structural units (phases) of the samples, i.e., on segregated or newly developed reduced copper surface and on oxidized alloying elements. It is interesting to note the tendencies and relations of the changes in surface copper and carbon content (Table 4). The concentration of copper of the samples after reaction in helium is always rather low, whereas the carbon content is usually the highest. Reaction in hydrogen brings about a significant increase in the copper content with the concomitant decrease in surface carbon concentration. The scaling, however, may not be linear due to the effects described above.

The majority of oxygen contamination with the O1s signal at about 530 eV is bound to the metallic components of the alloy. Again, a few percent is bonded to the surface carbon contaminant in either ether, ketone, carboxylic, or carbonate type bonds well distinguishable as high binding energy components of the O1s signal.

Surface contaminants are expected to affect most significantly the accuracy of the analysis of copper, since the Cu2p signal recorded at about 320 eV kinetic energy has the lowest energy of the measured elements. The low kinetic energy of the Cu2p line results in a relatively low penetration depth of this signal

TABLE 4: Surface Composition and Chemical States of Copper (Atomic %) on the Surface of Alloy Samples in the As-Received State and after Reactions

		Cu−Ti				Cu−Zr				Cu−Hf		
		as received	in He[a]	in H_2[b]		as received	in He[a]	in H_2[b]		as received	in He[a]	in H_2[b]
Cu		17.1	2.9	21.1		10.3	13.8	22.8		12.1	17.1	29.2
	Cu^0	0	0	0[c]		3.5	3.5	5.2		1.0	6.0	5.9
	Cu^+	2.1	0.7	1.5		4.8	9.2	10.7		1.5	11.1	13.4
	Cu^{2+}	15.0	2.2	19.6		2.0	1.1	6.9		9.6	0	9.9
M	Ti	12.5	12.6	9.5	Zr	15.2	13.1	10.6	Hf	7.3	4.3	4.4
									Zr	13.8	19.6	1.3
O		37.7	34.8	42.6		41.5	37.5	37.5		29.3	22.5	32.7
C		32.7	49.7	26.8		33.0	35.6	29.1		37.5	36.5	32.4

[a] 100 mg of sample, 2-propanol, 573 K, 24 h. [b] 100 mg of sample, 2-propanol, 523 K, 24 h. [c] Detectable.

through the carbon contamination and reaction product layer. Copper concentrations consequently may be underestimated. If one considers, however, that the concentration of the contaminants, although it changes from sample to sample, is always comparatively high in all samples, the data obtained for copper can be used for comparative purposes.

Evaluation of the Chemical State of the Constituents. *The Chemical State of Copper*. XPS characterization of the catalysts performed before and after the catalytic reactions permitted us to determine the chemical states of copper. The catalysts were cooled to room temperature in the atmosphere of the catalytic mixture and the carrier gas of the reaction. Air exposure of the surface of the samples was unavoidable while transferring the samples from the catalytic reactor to the spectrometer.

Such handling often provokes speculations on posttreatment oxidation of metallic copper (and also Cu_2O), considered to be the principal active component in the reactions investigated. In fact, only a very thin Cu(I) oxide layer was observed to develop when a reduced Cu−ZnO catalyst was exposed to air at room temperature, and long exposure was needed to observe Cu^{2+} species.[6] In line with this, vacuum-annealed CuO with Cu_2O-like surface was not oxidized back to CuO by exposure of oxygen at 300 °C.[7] A short, e.g., a few-minute, exposure to air of completely reduced samples does not show considerable change in the oxidation state of copper. In contrast, partial reduction of oxidized CuO and Cu_2O surfaces was brought about by prolonged vacuum annealing.[8] This reaction is also promoted by UV irradiation. Reduction of copper oxides due to direct heating to 100−200 °C or X-ray exposure under vacuum, especially in the presence of carbonaceous compounds, has been discussed for a long time.[9]

In light of the above literature observations (together with the experience of the present authors with supported Cu and Cu/ZnO catalysts), we can conclude that the presence of Cu^0, Cu^+, and Cu^{2+} oxidation states of these alloy catalysts can be determined with high confidence, although the accuracy of the $Cu/Cu_2O/CuO$ values may be slightly affected by the discussed oxidation−reduction processes.

Characteristic XPS data are presented in Figures 3 and 4 for Cu−Zr exhibiting the best catalytic properties. The figures show the Cu2p and Zr3d lines determined for the original, as-prepared alloy powder and those used in reactions in helium or hydrogen. Peak fitting procedure was performed for each line as described in detail in the Experimental Section. For the Cu−Zr catalyst the results are shown in Figure 5, whereas all relevant numerical data for the species identified with the corresponding binding energies and kinetic energies are collected in Table 5. The most striking feature of these observations is that whereas Cu−Zr and Cu−Hf always contain a substantial amount of fully reduced copper (Cu^0 species) on their surface, only Cu^+ and Cu^{2+} could be detected on Cu−Ti (Table 4).

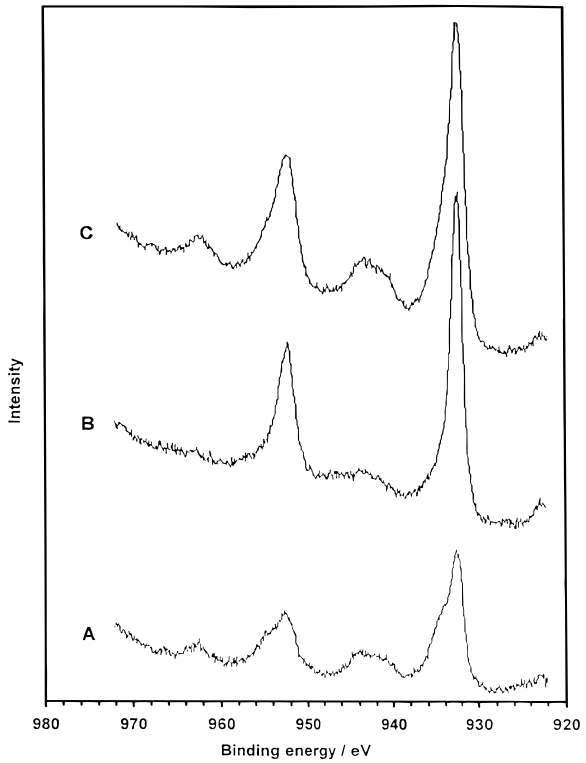

Figure 3. Cu2p region of the XPS spectrum of the Cu−Zr amorphous alloy powder. A, as received; B, used in the dehydrogenation of 2-propanol in helium (573 K, 24 h); C, used in the dehydrogenation of 2-propanol in hydrogen (523 K, 24 h).

The Chemical State of Ti, Zr, and Hf. In general, the chemical state of the second metal in the alloy systems used in this study, similar to Cu, is complex.

Surface titanium in the as-received Cu−Ti sample exists mostly in the oxidized state dominantly as Ti^{4+} and Ti^{3+} with a small contribution of Ti^{2+}. The surface after reaction in either helium or hydrogen becomes even more oxidized: the relative amount of Ti^{4+} increases significantly and Ti^{2+} almost completely disappears. The chemical state of zirconium of the as-received Cu−Zr alloy powder and that used in hydrogen are very similar with Zr^{3+} as the dominant species.[10−12] After reaction in helium, the surface again becomes more oxidized containing Zr^{4+} almost exclusively. Our findings are in accordance with a recent detailed study of various Zr-containing bicomponent amorphous alloys exposed to CO_2/H_2 or CO/H_2 reactant gas mixtures, where Zr^{4+} and various zirconium suboxides were found in the surface layer.[10]

The spectra of the Cu−Hf samples are more complex and rather difficult to interpret since reliable literature data do not exist. Nevertheless, the contribution of four chemical states are

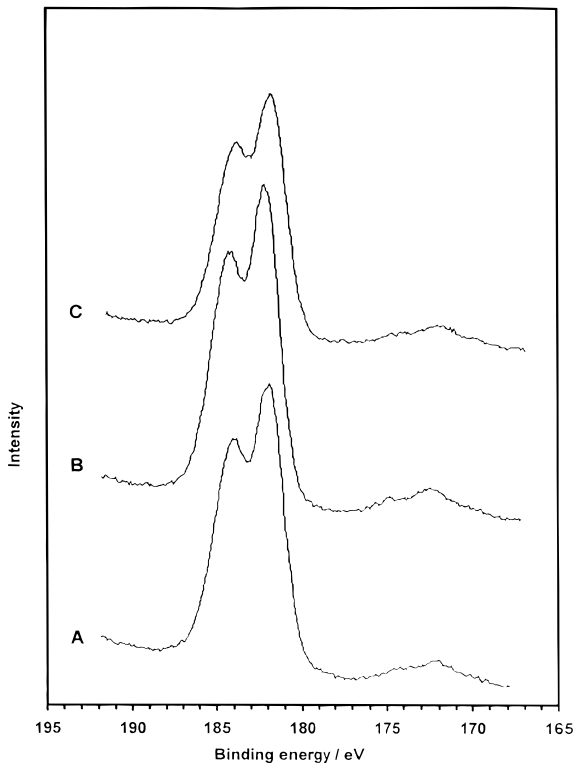

Figure 4. Zr3d region of the XPS spectrum of the Cu−Zr amorphous alloy powder (A−C are the same as in Figure 3).

evident. Hf^{2+} and Hf^{3+} species appear to dominate on the surface[13] (Table 5) with minor contributions of species with about 210 eV (Hf^0) and 215 eV (Hf^{4+}). Due to the lack of reliable literature information, however, these can only be considered as tentative assignments.[14] The zirconium impurity in Cu−Hf behaves exactly as zirconium does in Cu−Zr: Zr^{3+} (as-received and the sample used in hydrogen) or Zr^{4+} (sample used in helium) are the characteristic species.

Discussion

Surface Segregation Phenomena. One of the prominent findings of this study is the observation of substantial alterations of surface composition during the preparation and catalytic application of the amorphous alloy powders. Such phenomena are often described in the literature; detailed studies, however, are lacking.

The amorphization paths induced by mechanical alloying from the powders of the parent elements may depend on the preparation conditions and procedures. Local structure arrangements together with the general tendency of surface segregation toward reduction of the surface energy of the particles may lead to surface segregation of one or another component even in chemically neutral (high purity argon) ambient conditions (intrinsic segregation). The surface segregation may be related to bulk concentrations (eq 1) where Q is the heat of segregation and C_A and C_B are the concentrations of the constituent elements.[15,16]

$$\frac{(C_A/C_B)^S}{(C_A/C_B)^B} = \exp\left(-\frac{Q}{kT}\right) \tag{1}$$

A quantitative estimation of the intrinsic, thermodynamically driven (so-called Gibbsian) segregation can be estimated according to eq 2 (where γ_i is the surface tension and a_i is the relative area occupied by the particular type of atoms along a selected plane in the bulk). Spontaneous compositional change is directed toward lowering the overall surface energy resulting in negative Q values. When tabulated data of γ values for Cu ($\gamma = 1.934$), Ti ($\gamma = 2.570$), Zr ($\gamma = 2.700$), and Hf ($\gamma = 3.333$)[17] are used for calculations, the condition satisfies the enrichment of the surface in Cu for all three alloys considered.

$$Q = (\gamma_A a_A - \gamma_B a_B) \tag{2}$$

The lattice strain theory,[18] in contrast, predicts the segregation of the second metal in all cases (the atomic radius for copper is 128 pm, and for titanium, zirconium, and hafnium the radii are 147, 160, and 159 pm, respectively).

The Cu/M ratio on the surface in the as-prepared state and after catalytic reaction (Table 3) shows significant alteration in both directions from the nominal bulk values. Moreover, the predicted tendencies discussed above, i.e., either Cu enrichment or the enrichment of the surface in the second metal, can only be expected in case the constituents are in the metallic state. In reactive environments, segregation of the more reactive alloy component does take place. Although numerous examples of such segregation phenomena are known, of the three alloys used in the present study, data are available mainly for Cu−Zr due to its application as a catalyst material. Some information is also found for Cu−Ti, which is due to its potential use as hydrogen storage material.

In an oxidizing environment, the affinity to oxygen prevails resulting in the selective oxidation and surface segregation of the more reactive component (Ti, Zr, or Hf). Preferential oxidation of Zr and Zr enrichment on the surface takes place upon oxygen exposure of amorphous Cu−Zr alloys of various compositions.[19] Oxygen, either dissolved or present as a tertiary suboxide in Cu-rich alloys, also induces surface segregation of Zr with the formation of ZrO_2 when crystalline samples are annealed in ultrahigh vacuum.[20] Formation of zirconium oxide was similarly observed when a rapidly quenched amorphous $Cu_{30}Zr_{70}$ alloy was exposed to CO_2/H_2 or CO/H_2 reactant gas mixtures at 523 K.[10] Oxidation of Zr occurs despite a large excess of hydrogen, indicating that the zirconium component is highly reactive toward the carbon oxides. In sharp contrast, massive segregation of copper with the concomitant oxidation of zirconium was observed with the $Cu_{70}Zr_{30}$ system.[10]

The results of hydrogen-induced surface segregation of Cu−Zr alloys are rather controversial. Strong Cu segregation after annealing crystalline copper-rich alloys in hydrogen was reported.[20] No significant change in surface composition was measured, however, when amorphous $Cu_{30}Zr_{70}$ and crystalline $Cu_{30}Zr_{70}$ and $Cu_{70}Zr_{30}$ were treated with hydrogen (473 K, 16 h).[21] In contrast, a thick Cu-enriched layer was formed at the surface of the amorphous $Cu_{70}Zr_{30}$ alloy ribbon upon the same hydrogen treatment. The specimen thus prepared contained small copper particles embedded in a zirconia matrix. Rapidly quenched Cu−Zr amorphous alloy ribbons also undergo significant copper segregation when used as a catalyst in the dehydrogenation of alcohols.[22,23] We note here that, in the latter cases, differences were detected even between the characteristics of the inner side of the ribbons (the side that was in contact with the rotating wheel during the rapid quenching process) and the outer surface (also called the free-surface side).

Naturally, the discussed segregation phenomena are accompanied by substantial bulk and surface chemical changes. The significance of these transformations is the generation of highly active and stable catalytic materials from amorphous alloy precursors. Examples of such applications are numerous

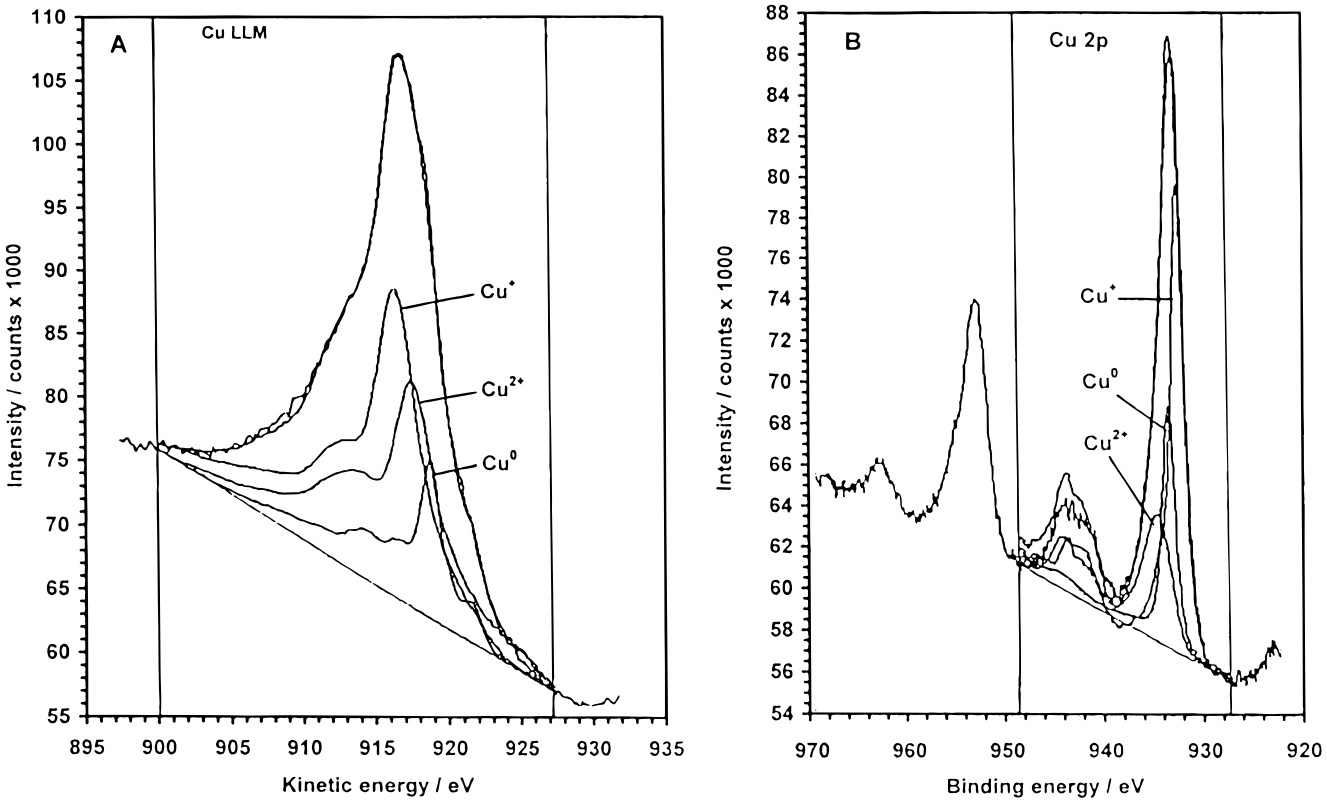

Figure 5. Cu(LMM) (A) and Cu2p (B) region of the XPS spectrum of the Cu−Zr amorphous alloy powder used in the dehydrogenation of 2-propanol in hydrogen (523 K, 24 h). Also shown are the best fit and the contribution of the individual copper species.

TABLE 5: Binding and Kinetic Energies of Electrons Corresponding to Surface Species of Alloy Samples in the As-Received State and after Reactions

	Cu−Ti					Cu−Zr					Cu−Hf				
	Cu2p BE (eV)		Cu(LMM) KE (eV)	Ti2p BE (eV)		Cu2p BE (eV)		Cu(LMM) KE (eV)	$Zr3d_{5/2}$ BE (eV)		Cu2p BE (eV)		Cu(LMM) KE (eV)	$Hf4d_{5/2}$[d] BE (eV)	
as received	Cu^0			Ti^{2+}	455.1	Cu^0	932.6	918.6			Cu^0	932.6	918.8		
	Cu^+	932.4	916.3	Ti^{3+}	456.8	Cu^+	932.0	916.3	Zr^{3+}	181.7	Cu^+	931.8	916.5	Hf^{2+}	212.3
	Cu^{2+}	933.8	917.3	Ti^{4+}	458.3	Cu^{2+}	934.2[e]	917.3	Zr^{4+}	182.6	Cu^{2+}	933.9	917.5	Hf^{3+}	214.0
in He[a]	Cu^0	932.6	—[c]			Cu^0	932.9	918.7			Cu^0	932.7	918.9		
	Cu^+	932.3	—[c]			Cu^+	932.3	916.6			Cu^+	932.4	916.7	Hf^{2+}	212.5
	Cu^{2+}	933.7	—[c]	Ti^{4+}	458.4	Cu^{2+}	934.2[e]	918.0	Zr^{4+}	182.1	Cu^{2+}			Hf^{3+}	214.0
in H_2[b]	Cu^0					Cu^0	933.0	918.9			Cu^0	932.5	918.8		
	Cu^+	932.1	916.7	Ti^{3+}	455.9	Cu^+	932.2	916.6	Zr^{3+}	181.5	Cu^+	932.0	916.5	Hf^{2+}	212.8
	Cu^{2+}	934.3[c]	917.1[e]	Ti^{4+}	458.3	Cu^{2+}	934.1[e]	917.7	Zr^{4+}	182.5	Cu^{2+}	933.7	917.3[c]	Hf^{3+}	214.3

[a] 100 mg of sample, 2-propanol, 573 K, 24 h. [b] 100 mg of sample, 2-propanol, 523 K, 24 h. [c] Fitting, in this case, could not be made to a reasonable accuracy. [d] Tentative assignments. [e] Slightly higher values are possibly due to carbonate and hydoxy species.

especially for Zr-containing binary alloys including Fe−Zr (ammonia synthesis[24]), Ni−Zr (hydrogenation of CO_2,[10,25] CO,[10] and unsaturated aldehydes[26]), Pd−Zr (hydrogenation of CO_2,[10,27,28] CO,[10] and unsaturated aldehydes[26] and oxidation of CO[29,30]), Cu−Zr (hydrogenation of 1,3-butadiene,[31] CO_2,[10,32] and CO[10] and transformation of alcohols[22,23,33,34]), and Au−Zr (hydrogenation of CO_2[35]).

As is clear from the above discussion, the generation of the active catalyst from an amorphous alloy precursor is a complex process. In our case, the chemical changes taking place under reaction conditions may include oxidation of Ti, Zr, and Hf and the formation of their hydrides. In inert atmosphere, oxidation is the main chemical transformation induced by oxygen impurities in the feed (gas stream and reacting organic liquids), traces of water formed in dehydration of the reacting alcohols, and oxygen that is present in the alloy. In addition, oxygen-containing compounds (the starting alcohols and reaction intermediates) chemisorbing at metal sites through their oxygen atom may undergo deoxygenation, which also contributes to surface oxidation. Hydride formation becomes a major factor contributing to the changes taking place when reactions are carried out in the presence of hydrogen.

Since all these processes take place at elevated (reaction) temperature, they bring about substantial changes in the bulk: the alloys are destabilized and phase separation occurs. The characteristic changes accordingly are the partial or complete crystallization of the amorphous alloys (see XRD data in Figure 1 and earlier DSC results[1]) even though reaction temperatures are well below the crystallization temperature of the alloys (697 K for Cu−Ti, 772 K for Cu−Zr, and 855 K for Cu−Hf). The main components of the formed specimens are copper and the corresponding oxides of the second metal. In addition, surface copper enrichment (Table 3) is evidenced in all cases with the most prominent change taking place with Cu−Hf where about a 10-fold increase is detected. These chemical and structural

changes, eventually, result in high catalytic activities in the transformations of alcohols.

The exceptional behavior of Cu−Ti in inert (helium) atmosphere, which is different from that of Cu−Zr and Cu−Hf, needs to be interpreted. As it is seen from the XRD curves (Figure 1), phase separation does not occur in this case, but Cu−Ti is transformed into various intermetallic compounds ($CuTi_2$ and γ-CuTi). They undergo neither oxidation in the bulk as it happened to Zr and Hf nor further transformations (like precipitation of metallic Cu phase) under the reaction conditions applied. According to XPS results, however, the surface is composed primarily of titanium species. Titanium segregation is in accordance with lattice strain theory, and partial oxidation also acts in the same direction. This phenomenon, however, may be a simple composition effect. As it was pointed out above, copper segregation of Cu−Zr alloys is usually observed at the copper-rich end of alloy composition.[20,21] Since our Cu−Ti sample is rich in titanium, titanium enrichment may be expected.

The existence of $CuTi_2$ and γ-CuTi nuclei, already present in the amorphous matrix acting as heterogeneous nucleation centers, was invoked to explain a noticeable lowering of the crystallization temperature in amorphous Cu−Ti powders prepared by mechanical alloying in comparison with that observed in melt spun ribbons of similar composition.[36,37] Therefore, the temperature at which the reaction was carried out under He (573 K) is high enough to start the nucleation and growth of the intermetallic phases observed at the end of the 24-h reaction as shown in Figure 1. Since Cu is used up completely in the formation of the equilibrium intermetallic compounds ($CuTi_2$ and γ-CuTi), the lack of metallic Cu limits the alcohol activation as manifested by the low conversions characteristic of Cu−Ti specimen.

On the contrary, copper formation is the main process for the Cu−Zr and Cu−Hf systems. In these latter cases, the oxide formation that is due to oxidation processes of Zr and Hf (oxygen impurities and alcohol dissociation) is an additional driving force toward Cu demixing from the matrix. The presence of ZrH_2 is to be also related to the dissociation of alcohol, and it is probably formed at the expense of acidic hydrogen of the alcohol.

In hydrogen atmosphere two parallel, competing mechanisms were observed for the Cu−Ti system. One still concerns the crystallization of the equilibrium $CuTi_2$ and γ-CuTi compounds, whereas the other is related to the formation of TiH_2. This latter one is the main process as indicated by the most intense peaks in the XRD pattern, whereas the $CuTi_2$ signals appear as shoulders on the TiH_2 and Cu peaks. DSC results (not shown) confirm these findings showing an intense exothermic peak related to hydrogen evolution from TiH_2. The mobility of hydrogen and its affinity to Ti induces the structural reconstruction of the amorphous, metastable matrix leading to the formation of the crystalline TiH_2 phase. In this phase, tetrahedral topological sites are occupied by four Ti atoms with hydrogen occupying the cavities of the tetrahedron. A Ti depletion obviously results with the concomitant observed Cu demixing. It appears however that, in the presence of hydrogen, the difference between the surface composition of the alloys disappears, i.e., Cu−Ti behaves like the other two alloys. Apparently, the hydrogen-induced phase separation becomes the major driving force for structural changes in both cases.

The Chemical State of Copper. Another striking feature of the behavior of the alloys studied is the marked difference found between the chemical states of copper of Cu−Ti and the other two alloys. According to literature data, either metallic copper (Cu^0)[38,39] is involved in the dehydrogenation of alcohols to carbonyl compounds or the coexistence of metallic and oxidized copper species[40,41] is required. On the basis of these observations as well as the inactivity of Cu−Ti alloy in such dehydrogenations, the lack of surface Cu^0 could be predicted.[1] This is, indeed, what is observed: no Cu^0 was ever detected on Cu−Ti after reactions (results of in situ measurements in Table 1), but either Cu^+ or Cu^{2+} was found to be the dominant species (XPS results in Table 4). On Cu−Zr and Cu−Hf, in contrast, large Cu^0 surface areas were measured by N_2O titration (Table 1). In accordance with this, a substantial fraction of surface copper was still in the reduced state as determined by XPS (Table 4), despite the fact that the samples were exposed to air before these latter measurements.

As an important point, the interrelation of Cu^0 values determined by N_2O titration and XPS analysis should be discussed here. When appropriately executed, N_2O titration only measures the number of surface Cu^0 atoms, whereas XPS is able to probe a few atomic layers. In addition, N_2O titration was carried out in situ after reactions, whereas the samples were removed from the reactor before XPS measurements. This naturally affects surface compositions resulting in a decrease in the Cu^0 concentrations. This is the main reason Cu^0 concentration values measured by XPS do not show the same significant increases after reaction in hydrogen as those determined by N_2O titration. Nevertheless, as discussed above, XPS still allows the determination of oxidation states of copper with high confidence.

XRD again provides further valuable information to interpret the differences observed in the behavior of the three speciemens. As mentioned, Cu demixing and oxidation of the second metal are parallel processes when Cu−Zr and Cu−Hf are used in reactions. Due to the reaction conditions applied, the newly segregated Cu exists in the metallic state not only in the bulk but also on the surface. With respect to Cu−Ti, Cu demixing does occur in the presence of hydrogen with the concomitant formation of TiH_2. Although titanium is found to be in the oxidized state on the surface, the underlying bulk titanium hydride phase is stable in the presence of hydrogen. This is strongly supported by the observation that, in contrast with the other two alloys, Cu−Ti used in hydrogen still contains a significant fraction of the amorphous state. It appears that under these conditions Cu acts as an oxygen scavenger and forms oxidized surface species, thus depressing the rate of dehydrogenation.

Conclusion

A combination of instrumental (XPS and XRD) studies and copper surface area measurements (N_2O titration) has allowed us to characterize the bulk and surface structural and compositional changes occurring when Cu−M amorphous alloy powders made by mechanical alloying are applied as catalyst materials. These changes are correlated with the results of catalytic studies to interpret fundamental differences observed in the catalytic performance of Cu−Ti versus Cu−Zr and Cu−Hf. Copper segregation and the presence of metallic copper on the surface found for Cu−Zr and Cu−Hf alloys correlate well with their high catalytic activity. In contrast, either stable intermetallic compounds $CuTi_2$ and γ-CuTi (when working in inert atmosphere) or oxidized copper and TiH_2 (when working in hydrogen) are the characteristic species found for Cu−Ti. We can therefore conclude that the negligible catalytic activity of this latter alloy is due to the fact that metallic copper does not exist on the surface.

Acknowledgment. Financial support by the Ministry of Culture and Education (Grant 137/96) is gratefully acknowledged. The XPS characterization was performed in the ESCA Surface Laboratory of the Budapest OTKA Measuring Center at the Research Laboratory of Materials and Environmental Chemistry.

References and Notes

(1) Molnár, Á.; Domokos, L.; Katona, T.; Martinek, T.; Mulas, G.; Cocco, G.; Bertóti, I.; Szépvölgyi, J. *Mater. Sci. Eng. A* **1997**, *226*−*228*, 1074.

(2) Wagner, C. D.; Riggs, W. M.; Davis, L. E.; Moulder, J. F.; Muilenberg, G. E. *Handbook of X-ray Photoelectron Spectroscopy*; Physical Electronics Division, Perkin-Elmer Corporation: Eden Prairie, MN, 1979.

(3) Moulder, J. F.; Stickle, W. F.; Sobol, P. E.; Bomben, K. D. *Handbook of X-ray Photoelectron Spectroscopy*; Physical Electronics Division, Perkin-Elmer Corporation: Eden Prairie, MN, 1992.

(4) Evans, J. W.; Wainwright, M. S.; Bridgewater, A. J.; Young, D. J. *Appl. Catal*. **1983**, *7*, 75.

(5) Denise, B.; Sneeden, R. P. A.; Beguin, B.; Cherifi, O. *Appl. Catal*. **1987**, *30*, 353.

(6) Okamoto, Y.; Fukino, K.; Imanaka, T.; Teranishi, S. *J. Phys. Chem*. **1983**, *87*, 3747.

(7) Goodby, B. E.; Pemberton, J. E. *Appl. Spectr*. **1988**, *42*, 754.

(8) Poulston, S.; Parlett, P. M.; Stone, P.; Bowker, M. *Surf. Interface Anal*. **1996**, *24*, 811.

(9) Klein, J. C.; Li, C. P.; Hercules, D. M.; Black, J. F. *Appl. Spectrosc*. **1984**, *38*, 727.

(10) Kilo, M.; Hund, M.; Sauer, G.; Baiker, A.; Wokaun, A. *J. Alloys Compd*. **1996**, *236*, 137.

(11) Wong, P. C.; Li, Y. S.; Zhou, M. Y.; Mitchell, K. A. R. *Appl. Surf. Sci*. **1995**, *89*, 255.

(12) Bertóti, I.; Kelly, R.; Mohai, M.; Tóth, A. *Nucl. Instrum. Methods Phys. Res*. **1993**, *B80/81*, 1219.

(13) Mitchell, D. F.; Sproule, G. I.; Graham, M. J. *Surf. Interface Anal*. **1990**, *15*, 487.

(14) Studies are under way to determine the exact chemical states of hafnium species and the accurate surface composition of the Cu−Hf alloy samples. Results will be published elsewhere.

(15) Abraham, F. F.; Tsai, N. H.; Pound, G. M. *Surf. Sci*. **1979**, *83*, 406.

(16) Wandelt, K.; Brundle, C. R. *Phys. Rev. Lett*. **1981**, *46*, 1529.

(17) Mezey, L.; Giber, J. *Jpn. J. Appl. Phys*. **1982**, *21*, 1569.

(18) Guy, A. G. *Introduction to Materials Science*; McGraw-Hill: New York, 1972.

(19) Sen, P.; Sarma, D. D.; Budhani, R. C.; Chopra, K. L.; Rao, C. N. R. *J. Phys. F: Met. Phys*. **1984**, *14*, 565.

(20) Yu, X.-N.; Schlapbach L. *Z. Phys. Chem. N. F*. **1989**, *164*, 1171.

(21) Vanini, F.; Büchler, St.; Yu, X.-N.; Erbudak, M.; Schlapbach L.; Baiker, A. *Surf. Sci*. **1987**, *189/190*, 1117.

(22) Katona, T.; Hegedûs, Z.; Kopasz, Cs.; Molnár, Á.; Bartók, M. *Catal. Lett*. **1990**, *5*, 361.

(23) Molnár, Á.; Katona, T.; Bartók, M.; Perczel, I. V.; Hegedûs, Z.; Kopasz, Cs. *Mater. Sci. Eng*. **1991**, *A134*, 1083.

(24) (a) Baiker, A.; Schlögl, R.; Armbruster, E.; Güntherodt, H. J. *J. Catal*. **1987**, *107*, 221. (b) Schlögl, R.; Wiesendanger, R.; Baiker, A. *J. Catal*. **1987**, *108*, 452.

(25) Schild, C.; Wokaun, A.; Koeppel, R. A.; Baiker, A. *J. Phys. Chem*. **1991**, *95*, 6341.

(26) Baiker, A.; De Pietro, J.; Maciejewski, M.; Walz, B. *Structure*−*Activity and Selectivity Relationships in Heterogeneous Catalysis*; Grasselli, R. K., Sleight, A. W., Eds.; Elsevier: Amsterdam, 1991. *Stud. Surf. Sci. Catal*. **1991**, *67*, 169.

(27) Baiker, A.; Gasser, D. *J. Chem. Soc., Faraday Trans.* **1989**, *85*, 999.

(28) Schild, C.; Wokaun, A.; Baiker, A. *J. Mol. Catal*. **1990**, *63*, 223.

(29) Baiker, A.; Gasser, D.; Lenzner, J.; Reller, A.; Schlögl, R. *J. Catal*. **1990**, *126*, 555.

(30) Gredig, S.; Tagliaferri, S.; Maciejewski, M.; Baiker, A. *Catalysis and Automotive Pollution Control III*; Frennet, A., Bastin, J.-M., Eds.; Elsevier: Amsterdam, 1995. *Stud. Surf. Sci. Catal*. **1995**, *96*, 285.

(31) Baiker, A.; Baris, H.; Erbudak, M.; Vanini, F. *New Frontiers in Catalysis*; Guczi, L., Solymosi, F., Tétényi, P., Eds.; Elsevier: Amsterdam, 1993. *Stud. Surf. Sci. Catal*. **1993**, *75*, 1928.

(32) Gasser, D.; Baiker, A. *Appl. Catal*. **1989**, *48*, 279.

(33) Martinek, T.; Molnár, Á.; Katona, T.; Bartók, M.; Lovas, A. *J. Mol. Catal. A: Chem.* **1996**, *112*, 85.

(34) Domokos, L.; Katona, T.; Molnár, Á.; Lovas, A. *Appl. Catal. A: Chem.* **1996**, *142*, 151.

(35) Koeppel, R. A.; Baiker, A.; Schild, C.; Wokaun, A. *J. Chem. Soc., Faraday Trans.* **1991**, *87*, 2821.

(36) Cocco, G.; Enzo, S.; Magini, M.; Cowlam, N. *Colloq. Phys*. **1990**, *C4*, 181.

(37) Politis, C.; Johnson, W. L. *J. Appl. Phys*. **1986**, *60*, 1147.

(38) Kanoun, N.; Astier, M. P.; Pajonk, G. M. *J. Mol. Catal.* **1993**, *79*, 217.

(39) Marchi, A. J.; Fierro, J. L. G.; Santamaría, J.; Monzón, A. *Appl. Catal. A: Chem.* **1996**, *142*, 375.

(40) Cunningham, J.; Al-Sayyed, G. H.; Cronin, J. A.; Healy, C.; Hirschwald, W. *Appl. Catal.* **1986**, *25*, 129.

(41) Cunningham, J.; Al-Sayyed, G. H.; Cronin, J. A.; Fierro, J. L. G.; Healy, C.; Hirschwald, W.; Ilyas, M.; Tobin, J. P. *J. Catal.* **1987**, *102*, 160.